Supplement of Atmos. Chem. Phys., 24, 4217–4229, 2024
https://doi.org/10.5194/acp-24-4217-2024-supplement

Supplement of

Reanalysis of NOAA H_2 observations: implications for the H_2 budget

Fabien Paulot et al.

Correspondence to: Fabien Paulot (fabien.paulot@noaa.gov)

S1 Supporting text

S1.1 Missing source estimate

Following Ghosh et al. (2015), the changes in the H_2 source ($\Delta S(H_2)$) needed to reduce the model bias ($\Delta H_2(sfc)$) can be estimated as:

$$\Delta S(\mathrm{H_2}) = K_1 \frac{d(\Delta \mathrm{H_2}(sfc))}{dt} + K_2 \Delta \mathrm{H_2}(sfc) \quad (1)$$

where K_1 is the ratio of the simulated H_2 burden to the simulated surface concentration of H_2, K_2 is the ratio of the simulated loss of H_2 to the simulated surface concentration of H_2, and $\Delta H_2(sfc)$ is the difference between observed and simulated H_2. Here $\Delta S(H_2)$ is estimated from the bias as background sites.

S1.2 REVISED anthropogenic emissions

In the BASE simulation, anthropogenic emissions are assumed to solely originate from combustion processes and calculated using time-invariant and source-specific H_2 to CO emission ratios (Table S1) that reflect the water–gas shift reaction.

The REVISED emission inventory incorporates a more detailed treatment of H_2 emission factors. In particular, we account for the difference between gasoline- and diesel-powered vehicles and for the increase in the H_2 to CO emission ratio associated with three-way catalytic converters (Bond et al., 2010, 2011). H_2 vehicular emissions are estimated using H_2:CO emissions ratio (Table S1) and ECLIPSEv6 CO region- and vehicle-type specific emissions (Klimont et al., 2017). These changes result in a model decrease in transportation emissions in 2010 (5.5 Tg/yr vs 5.8 Tg/yr).The REVISED emission ratio for biofuel and waste are from Andreae (2019). Following Vollmer et al. (2012), we assume that other residential emissions of CO (e.g., oil and gas stoves) do not produce H_2.

The industrial emission ratio is not modified between the BASE and REVISED emissions inventories. However, in the REVISED inventory, we use the Emissions Database for Global Atmospheric Research (EDGAR) v6.1 industrial CO emissions instead of CEDS to estimate industrial H_2 emissions. These inventories exhibit different trends for CO (+8.7 Tg/yr for EDGAR and -30.7 Tg/yr for CEDS in 2018 relative to 2010), which translate to different trends in H_2 emissions (+0.1 Tg/yr and -0.4 Tg/yr, respectively). We select the EDGAR inventory as we identified the decrease in industrial H_2 as one of the main drivers for the decline in anthropogenic emission in the BASE inventory.

The REVISED inventory also includes a non-combustion source of H_2 associated with H_2 industrial production (primarily for NH_3 production and refining (International Energy Agency, 2019)). H_2 release from such facility is uncertain due to the lack of sensing technology. Recent estimates range from 0% to 2.7% (Arrigoni and Bravo Diaz, 2022; Fan et al., 2022; Frazer-Nash Consultancy, 2022). Here we assume a 2% release rate (Bond et al., 2011), which yields an estimated source of 1.5 Tg/yr in 2010 and 1.8 Tg/yr in 2019.

S1.3 REVISED natural emissions

In the REVISED inventory, marine H_2 emissions are calculated interactively (Johnson, 2010; Paulot et al., 2021) from the simulated distribution of surface seawater CO (Conte et al., 2019), scaled to produce a net flux of 6 Tg/yr. We use CO as a proxy for biological activity following Pieterse et al. (2011). Relative to the BASE inventory, the REVISED inventory exhibits higher emissions in the tropics and lower emissions in the Southern ocean, which reflects changes in the solubility of H_2 (Fig. S3a).

The soil source of H_2 is distributed following the simulated land biological nitrogen fixation from the MIROC-ES2L Earth system model (Hajima et al., 2020). The soil H_2 flux is set to 4.5 Tg/yr, which is at the high end of previous estimates (Ehhalt and Rohrer, 2009). MIROC-ES2L explicitly accounts for biological nitrogen fixation by crops. This results in much larger H_2 emissions in the Northern mid latitudes relative to the BASE soil emissions.

Biomass burning emissions are kept unchanged from Paulot et al. (2021). However, we note that using the emission factors of Andreae (2019) would reduce H_2 emissions from 8.3 to 6.1 Tg/yr over the 2010–2019 period. This is less than previous estimates (10–20 Tg/yr) (Ehhalt and Rohrer, 2009; Andreae, 2019), which may partly reflect an underestimate in the global burned area in GFED4s (Chen et al., 2023).

S1.4 Deposition sensitivity

The deposition velocity of H_2 can be expressed as

$$\frac{1}{v_d(\mathrm{H_2})} = \frac{1}{g_i} + \frac{1}{g_s} \quad (2)$$

where g_i and g_s represent the H_2 conductance through barriers that reduce the transport of H_2 to active sites (e.g., canopy, litter, ...) and in the soil.

The conductance in the soil is expressed after Ehhalt and Rohrer (2013) as

$$g_s = \sqrt{k_m\, hT\, f\, D_s} \quad (3)$$

where hT and f are the sensitivity of H_2 biological uptake to temperature and soil moisture, respectively, D_s is the moisture-dependent diffusivity of H_2 in the soil, and k_m represents the maximum uptake rate of H_2. We assume that k_m is spatially invariant. All moisture dependencies are evaluated after Bertagni et al. (2021). Namely, f is expressed as

$$f(s) = \frac{1}{N}(s - s_{ws})^{\beta_1}(1 - s_{ws})^{\beta_2} \quad (4)$$

where s_{ws} is the threshold below which H_2 consumption is inhibited. s_{ws} can be estimated as:

$$s_{ws} = \left(\frac{\tilde{\Psi}}{\Psi_{ws}}\right)^{\frac{1}{b}} \quad (5)$$

where the $\tilde{\Psi}$ and b constants can be determined experimentally (Bertagni et al., 2021) and Ψ_{ws} is the soil matrix potential below which bacterial uptake is inhibited. Given s_{ws}, β_1 and β_2 can be estimated based on observational constraints (Bertagni et al., 2021).

For g_i, we account for the impact of canopy and above-ground litter. For the canopy, we assume a time-invariant conductance based on the vegetation type (Makar et al., 2018). The litter conductance is estimated assuming a litter porosity of 0.62 (Wang et al., 2019). The litter depth is estimated based on the simulated above ground carbon from the IPSL INCA model historical simulation (Boucher et al., 2021) assuming a density of 0.03 g/cm^3 (Chojnacky et al., 2009).

We carry sensitivity experiments in which the resistance due to litter and canopy conductance are scaled by a factor between 0 and 2 and Ψ_{ws} takes values between -10^5 and -10^3 kPa (compared to -3000 kPa in REVISED_GLDAS). For each combination, k_m is optimized to yield the same global $v_d(\mathrm{H_2})$ for year 2010. We find that the canopy resistance has little impact on the meridional gradient and trend and we focus our analysis on the litter resistance.

Fig. S6 shows the measured and simulated $v_d(\mathrm{H_2})$ at 7 different sites. As noted previously by Paulot et al. (2021), all parameterizations tend to overestimate the variability in $v_d(\mathrm{H_2})$ across sites. In particular, $v_d(\mathrm{H_2})$ is underestimated at Tsukuba and Mace Head (Fig. S6c and e). In contrast, seasonality and magnitude are well captured by all parameterizations at temperate sites (a, b, d, g). The large spread in simulated $v_d(\mathrm{H_2})$ at the San Jacinto Mountain Reserve (desert) reflects different degrees of inhibition of HA-HOBs under low soil moisture (Fig. S6f).

S2 Supporting tables and figures

Table S1: Sector-based molar H_2 to CO emission ratio

		BASE[a]	REVISED
Industrial		0.2	0.2
Residential			
	Biofuel	0.3	0.31 [b]
	Other	0.3	0 [c]
Transportation			
	Gasoline-powered vehicles (up to EURO3)	0.5	0.5 [d]
	Gasoline-powered vehicles (EURO4 and above)	0.5	1 [d]
	Diesel-powered vehicle	0.5	0.0021 [d]
	CNG-powered vehicle	0.5	0.04 [d]
Waste		0.07	0.32 [b]

[a] Paulot et al. (2021) [b] Andreae (2019) [c] Vollmer et al. (2012) [d] Bond et al. (2010, 2011)

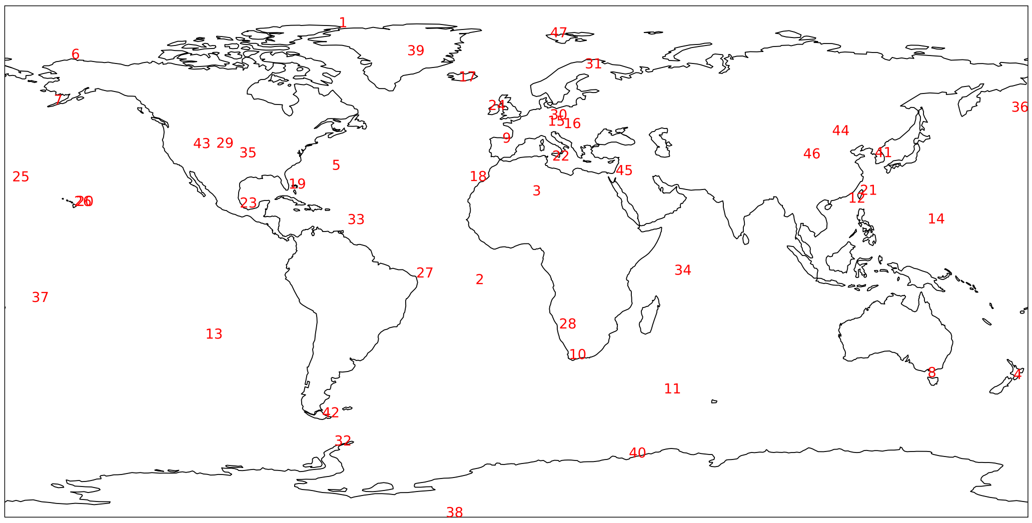

Figure S1: Location of the ground surface stations used in this study. 1.ALT 2.ASC 3.ASK 4.BHD 5.BMW 6.BRW 7.CBA 8.CGO 9.CIB 10.CPT 11.CRZ 12.DSI 13.EIC 14.GMI 15.HPB 16.HUN 17.ICE 18.IZO 19.KEY 20.KUM 21.LLN 22.LMP 23.MEX 24.MHD 25.MID 26.MLO 27.NAT 28.NMB 29.NWR 30.OXK 31.PAL 32.PSA 33.RPB 34.SEY 35.SGP 36.SHM 37.SMO 38.SPO 39.SUM 40.SYO 41.TAP 42.USH 43.UTA 44.UUM 45.WIS 46.WLG 47.ZEP. Further information regarding each station can be found at Global Monitoring Laboratory (2023)

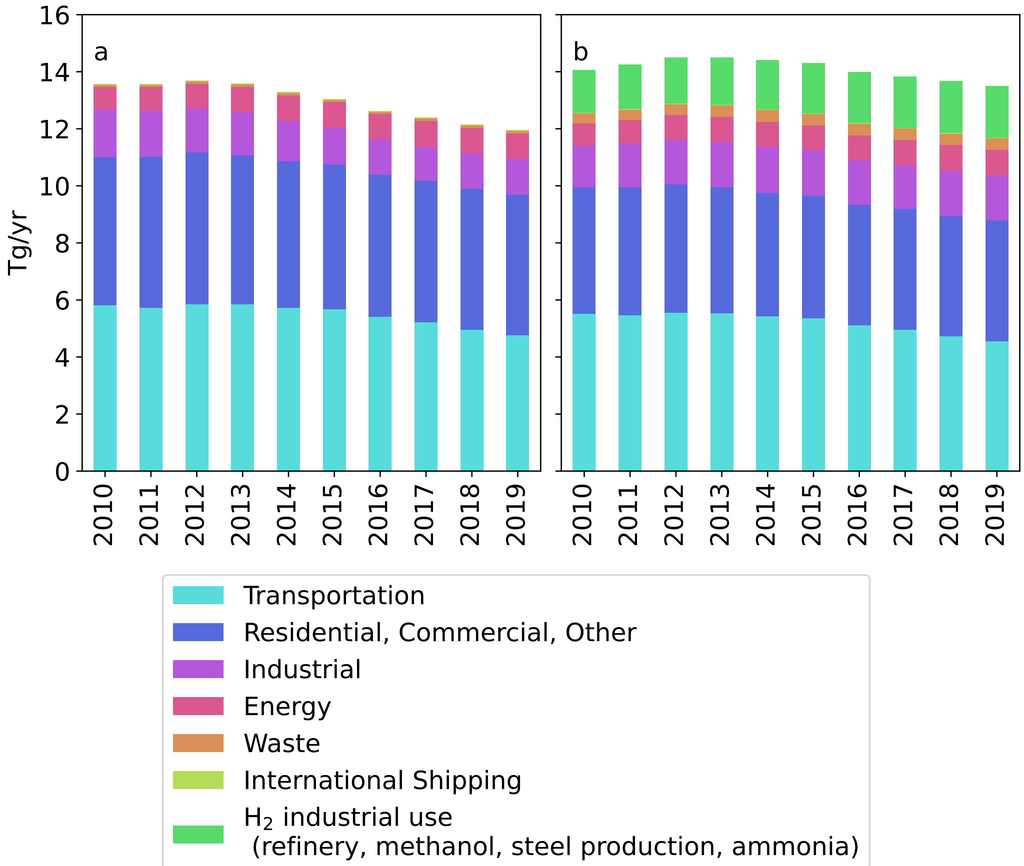

Figure S2: Sectorial H_2 anthropogenic emissions in the BASE (a) and REVISED (b) configurations

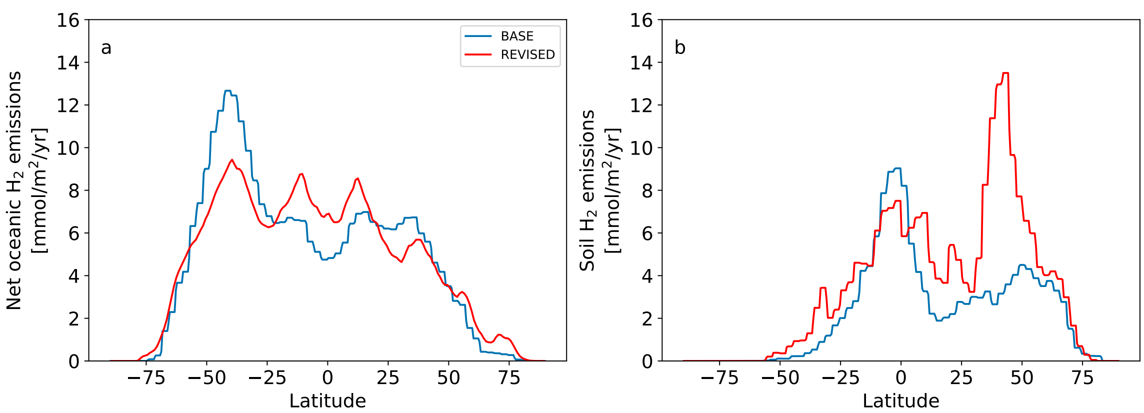

Figure S3: Marine and soil H_2 emissions in the BASE and REVISED emission inventories.

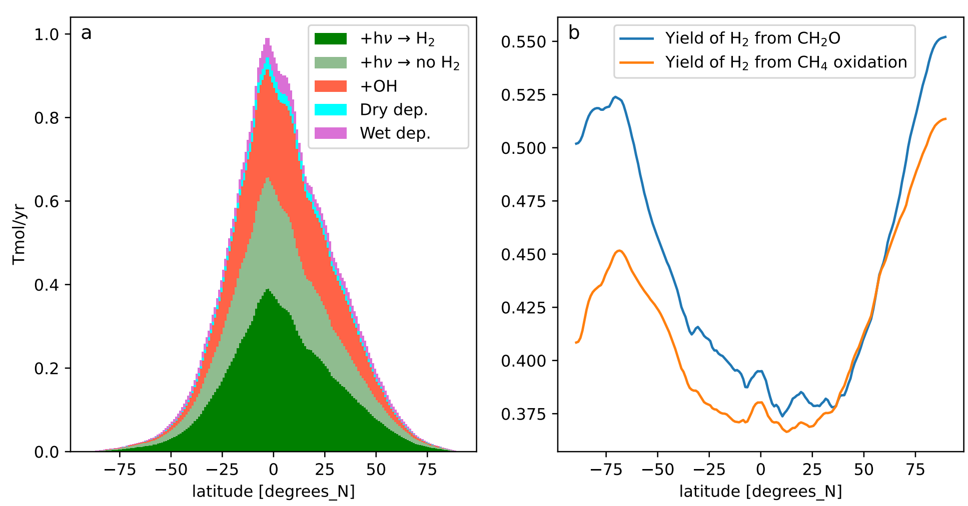

Figure S4: Simulated CH_2O loss (a) and H_2 yield from CH_2O and CH_4. The yields are estimated by dividing the 2010–2019 average column-integrated H_2 production associated with CH_2O and CH_4 photooxidation by the column-integrated chemical and depositional loss of CH_2O and by the phochemical loss of CH_4, respectively.

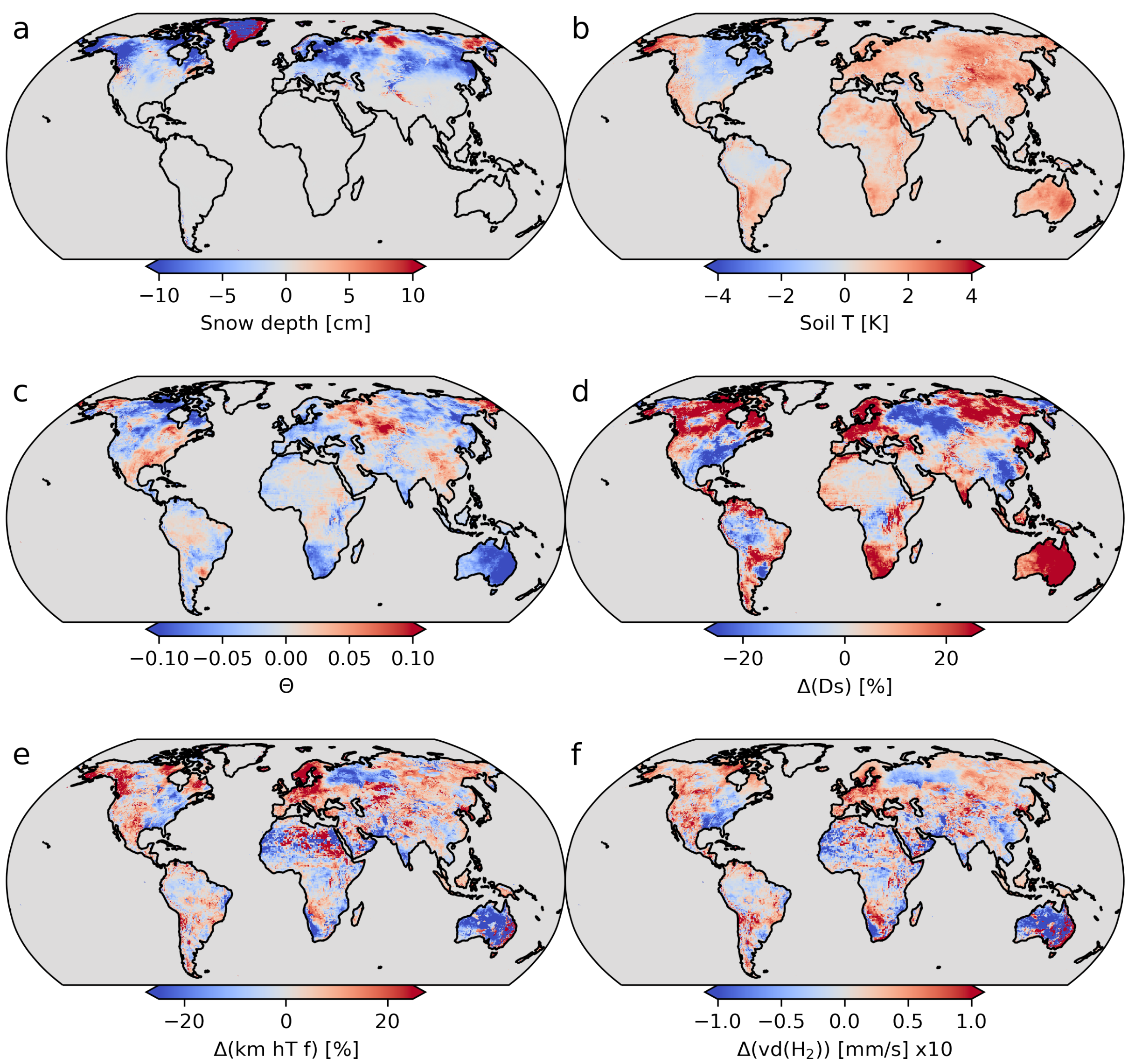

Figure S5: Changes in snow depth (a), soil temperature (b), soil moisture (as a fraction of pores (c)) and their impact on H_2 soil diffusivity (d), H_2 bacterial uptake, (e) and H_2 deposition velocity (REVISED_GLDAS, panel f) between years (2017–2019) and years (2010–2012).

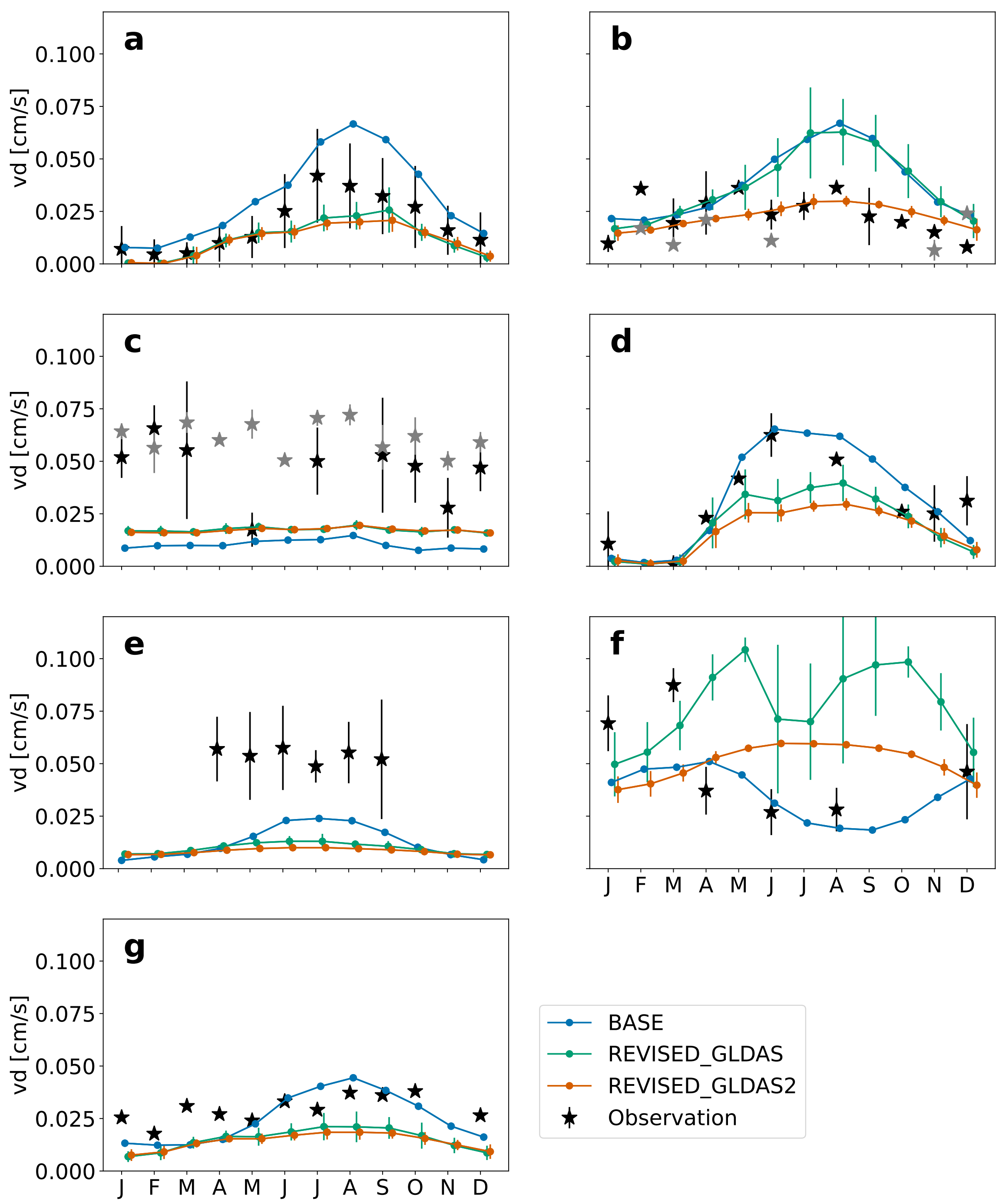

Figure S6: Comparison between simulated and observed H_2 deposition velocity at (a) Harvard Forest (temperate forest, (Meredith et al., 2016)), (b) Gif-sur-Yvette (pasture (Yver et al. (2009) (black); Belviso et al. (2013) (grey)), (c) Tsukuba (Yonemura et al. (2000) for agricultural land (black) and forest (grey)) (d) Helsinki (forest, Lallo et al. (2008)), (e) Mace Head (peat, Simmonds et al. (2011)) (f) San Jacinto Mountain Reserve (desert, Smith-Downey et al. (2008)), (g) Heidelberg (semi-urban, Hammer and Levin (2009)). Errorbars for the REVISED_GLDAS and REVISED_GLDAS2 configurations denote the standard deviation in the simulated monthly $v_d(H_2)$ over the 2010–2019 period.

References

Andreae, M. O.: Emission of trace gases and aerosols from biomass burning – an updated assessment, Atmospheric Chemistry and Physics, 19, 8523–8546, https://doi.org/10.5194/acp-19-8523-2019, 2019.

Arrigoni, A. and Bravo Diaz, L.: Hydrogen emissions from a hydrogen economy and their potential global warming impact: summary report of the Clean Hydrogen Joint Undertaking expert workshop on the Environmental Impacts of Hydrogen, JRC130362, https://doi.org/10.2760/065589, 2022.

Belviso, S., Schmidt, M., Yver, C., Ramonet, M., Gros, V., and Launois, T.: Strong similarities between night-time deposition velocities of carbonyl sulphide and molecular hydrogen inferred from semi-continuous atmospheric observations in Gif-sur-Yvette, Paris region, Tellus B: Chemical and Physical Meteorology, 65, 20 719, https://doi.org/10.3402/tellusb.v65i0.20719, 2013.

Bertagni, M. B., Paulot, F., and Porporato, A.: Moisture Fluctuations Modulate Abiotic and Biotic Limitations of H_2 Soil Uptake, Global Biogeochemical Cycles, 35, e2021GB006 987, https://doi.org/10.1029/2021gb006987, 2021.

Bond, S., Alvarez, R., Vollmer, M., Steinbacher, M., Weilenmann, M., and Reimann, S.: Molecular hydrogen (H2) emissions from gasoline and diesel vehicles, Science of The Total Environment, 408, 3596–3606, https://doi.org/10.1016/j.scitotenv.2010.04.055, 2010.

Bond, S., Gül, T., Reimann, S., Buchmann, B., and Wokaun, A.: Emissions of anthropogenic hydrogen to the atmosphere during the potential transition to an increasingly H_2-intensive economy, International Journal of Hydrogen Energy, 36, 1122–1135, https://doi.org/10.1016/j.ijhydene.2010.10.016, 2011.

Boucher, O., Denvil, S., Levavasseur, G., Cozic, A., Caubel, A., Foujols, M.-A., Meurdesoif, Y., Balkanski, Y., Checa-Garcia, R., Hauglustaine, D., Bekki, S., and Marchand, M.: IPSL IPSL-CM6A-LR-INCA model output prepared for CMIP6 CMIP historical, https://doi.org/10.22033/ESGF/CMIP6.13601, 2021.

Chen, Y., Hall, J., van Wees, D., Andela, N., Hantson, S., Giglio, L., van der Werf, G. R., Morton, D. C., and Randerson, J. T.: Multi-decadal trends and variability in burned area from the fifth version of the Global Fire Emissions Database (GFED5), Earth System Science Data, 15, 5227–5259, https://doi.org/10.5194/essd-15-5227-2023, 2023.

Chojnacky, D., Amacher, M., and Gavazzi, M.: Separating Duff and Litter for Improved Mass and Carbon Estimates, Southern Journal of Applied Forestry, 33, 29–34, https://doi.org/10.1093/sjaf/33.1.29, 2009.

Conte, L., Szopa, S., Séférian, R., and Bopp, L.: The oceanic cycle of carbon monoxide and its emissions to the atmosphere, Biogeosciences, 16, 881–902, https://doi.org/10.5194/bg-16-881-2019, 2019.

Ehhalt, D. and Rohrer, F.: Deposition velocity of H_2: a new algorithm for its dependence on soil moisture and temperature, Tellus B: Chemical and Physical Meteorology, 65, 19 904, https://doi.org/10.3402/tellusb.v65i0.19904, 2013.

Ehhalt, D. H. and Rohrer, F.: The tropospheric cycle of H_2: a critical review, Tellus B: Chemical and Physical Meteorology, 61, 500–535, https://doi.org/10.1111/j.1600-0889.2009.00416.x, 2009.

Fan, Z., Sheerazi, H., Bhardwaj, A., Corbeau, A.-S., Longobardi, K., Castañeda, A., Merz, A.-K., Woodall, C. M., Agrawal, M., Orozco-Sanchez, S., and Friedmann, J.: Hydrogen Leakage: A Hydrogen Leakage: A Potential Risk for the Hydrogen Economy, URL `https://www.energypolicy.columbia.edu/publications/hydrogen-leakage-potential-risk-hydrogen-economy/`, 2022.

Frazer-Nash Consultancy: Fugitive Hydrogen Emissions in a Future Hydrogen Economy - FNC 012865-53172R Issue 1, Tech. rep., UK Department for Energy Security and Net Zero, 2022.

Ghosh, A., Patra, P. K., Ishijima, K., Umezawa, T., Ito, A., Etheridge, D. M., Sugawara, S., Kawamura, K., Miller, J. B., Dlugokencky, E. J., Krummel, P. B., Fraser, P. J., Steele, L. P., Langenfelds, R. L., Trudinger, C. M., White, J. W. C., Vaughn, B., Saeki, T., Aoki, S., and Nakazawa, T.: Variations in global methane sources and sinks during 1910–2010, Atmospheric Chemistry and Physics, 15, 2595–2612, https://doi.org/10.5194/acp-15-2595-2015, 2015.

Global Monitoring Laboratory: Carbon Cycle Gases observation sites, URL `https://www.gml.noaa.gov/dv/site/?program=ccgg`, 2023.

Hajima, T., Watanabe, M., Yamamoto, A., Tatebe, H., Noguchi, M. A., Abe, M., Ohgaito, R., Ito, A., Yamazaki, D., Okajima, H., Ito, A., Takata, K., Ogochi, K., Watanabe, S., and Kawamiya, M.: Development of the MIROC-ES2L Earth system model and the evaluation of biogeochemical processes and feedbacks, Geoscientific Model Development, 13, 2197–2244, https://doi.org/10.5194/gmd-13-2197-2020, 2020.

Hammer, S. and Levin, I.: Seasonal variation of the molecular hydrogen uptake by soils inferred from continuous atmospheric observations in Heidelberg, southwest Germany, Tellus B: Chemical and Physical Meteorology, 61, 556–565, https://doi.org/10.1111/j.1600-0889.2009.00417.x, 2009.

International Energy Agency: The Future of Hydrogen – Seizing today's opportunities, Tech. rep., International Energy Agency, Paris, France, URL `https://www.iea.org/reports/the-future-of-hydrogen`, 2019.

Johnson, M. T.: A numerical scheme to calculate temperature and salinity dependent air-water transfer velocities for any gas, Ocean Sci., 6, 913–932, 2010.

Klimont, Z., Kupiainen, K., Heyes, C., Purohit, P., Cofala, J., Rafaj, P., Borken-Kleefeld, J., and Schöpp, W.: Global anthropogenic emissions of particulate matter including black carbon, Atmospheric Chemistry and Physics, 17, 8681–8723, https://doi.org/10.5194/acp-17-8681-2017, 2017.

Lallo, M., Aalto, T., Laurila, T., and Hatakka, J.: Seasonal variations in hydrogen deposition to boreal forest soil in southern Finland, Geophysical Research Letters, 35, https://doi.org/10.1029/2007gl032357, 2008.

Makar, P. A., Akingunola, A., Aherne, J., Cole, A. S., Aklilu, Y., Zhang, J., Wong, I., Hayden, K., Li, S.-M., Kirk, J., Scott, K., Moran, M. D., Robichaud, A., Cathcart, H., Baratzedah, P., Pabla, B., Cheung, P., Zheng, Q., and Jeffries, D. S.: Estimates of exceedances of critical loads for acidifying deposition in Alberta and Saskatchewan, Atmospheric Chemistry and Physics, 18, 9897–9927, https://doi.org/10.5194/acp-18-9897-2018, 2018.

Meredith, L. K., Commane, R., Keenan, T. F., Klosterman, S. T., Munger, J. W., Templer, P. H., Tang, J., Wofsy, S. C., and Prinn, R. G.: Ecosystem fluxes of hydrogen in a mid-latitude forest driven by soil microorganisms and plants, Global Change Biology, 23, 906–919, https://doi.org/10.1111/gcb.13463, 2016.

Paulot, F., Paynter, D., Naik, V., Malyshev, S., Menzel, R., and Horowitz, L. W.: Global modeling of hydrogen using GFDL-AM4.1: Sensitivity of soil removal and radiative forcing, International Journal of Hydrogen Energy, 46, 13 446–13 460, https://doi.org/10.1016/j.ijhydene.2021.01.088, 2021.

Pieterse, G., Krol, M. C., Batenburg, A. M., Steele, L. P., Krummel, P. B., Langenfelds, R. L., and Röckmann, T.: Global modelling of H_2 mixing ratios and isotopic compositions with the TM5 model, Atmospheric Chemistry and Physics, 11, 7001–7026, https://doi.org/10.5194/acp-11-7001-2011, 2011.

Simmonds, P., Derwent, R., Manning, A., Grant, A., O'doherty, S., and Spain, T.: Estimation of hydrogen deposition velocities from 1995-2008 at Mace Head, Ireland using a simple box model and concurrent ozone depositions, Tellus B: Chemical and Physical Meteorology, 63, 40–51, https://doi.org/10.1111/j.1600-0889.2010.00518.x, 2011.

Smith-Downey, N. V., Randerson, J. T., and Eiler, J. M.: Molecular hydrogen uptake by soils in forest, desert, and marsh ecosystems in California, Journal of Geophysical Research, 113, G03 037, https://doi.org/10.1029/2008jg000701, 2008.

Vollmer, M. K., Walter, S., Mohn, J., Steinbacher, M., Bond, S. W., Röckmann, T., and Reimann, S.: Molecular hydrogen (H_2) combustion emissions and their isotope (D/H) signatures from domestic heaters, diesel vehicle engines, waste incinerator plants, and biomass burning, Atmospheric Chemistry and Physics, 12, 6275–6289, https://doi.org/10.5194/acp-12-6275-2012, 2012.

Wang, H., van Eyk, P. J., Medwell, P. R., Birzer, C. H., Tian, Z. F., Possell, M., and Huang, X.: Air Permeability of the Litter Layer in Broadleaf Forests, Frontiers in Mechanical Engineering, 5, https://doi.org/10.3389/fmech.2019.00053, 2019.

Yonemura, S., Yokozawa, M., Kawashima, S., and Tsuruta, H.: Model analysis of the influence of gas diffusivity in soil on CO and H_2 uptake, Tellus B: Chemical and Physical Meteorology, 52, 919–933, https://doi.org/10.3402/tellusb.v52i3.17075, 2000.

Yver, C., Schmidt, M., Bousquet, P., Zahorowski, W., and Ramonet, M.: Estimation of the molecular hydrogen soil uptake and traffic emissions at a suburban site near Paris through hydrogen, carbon monoxide, and radon-222 semicontinuous measurements, Journal of Geophysical Research: Atmospheres, 114, https://doi.org/10.1029/2009jd012122, 2009.